Difluoroboron β-Diketonate Materials with Long-Lived Phosphorescence Enable Lifetime Based Oxygen Imaging with a Portable Cost Effective Camera

Alexander S. Mathew, **Christopher A. DeRosa**, **James N. Demas**, and **Cassandra L. Fraser**[*]

Department of Chemistry, University of Virginia, Charlottesville, Virginia 22904, USA

Abstract

Lifetime-based oxygen imaging is useful in many biological applications but instrumentation can be stationary, expensive, and complex. Herein, we present a portable, cost effective, simple alternative with high spatiotemporal resolution that uses a complementary metal oxide silicon (CMOS) camera to measure oxygen sensitive lifetimes on the millisecond scale. We demonstrate its compatibility with difluoroboron β-diketonate poly(lactic acid) (BF$_2$bdkPLA) polymers which are nontoxic and exhibit long-lived oxygen sensitive phosphorescence. Spatially resolved lifetimes of four BF$_2$bdkPLA variants are measured using nonlinear least squares (NLS) and rapid lifetime determination (RLD) both of which are shown to be accurate and precise. Real-time imaging in a dynamic environment is demonstrated by determining lifetime pixel-wise. The setup costs less than $5000, easily fits into a backpack, and can operate on battery power alone. This versatility combined with the inherent utility of lifetime measurements make this system a useful tool for a wide variety of oxygen sensing applications. This study serves as an important foundation for the development of dual mode real time lifetime plus ratiometric imaging with bright, long lifetime difluoroboron β-diketonate probes.

Introduction

Oxygen is essential to numerous biological processes and insufficient concentrations can cause physical ailments.[1] Consequently, quantification of oxygen has been of increasing interest for several decades. While there are many approaches to measuring oxygen, chemical probes displaying oxygen sensitive phosphorescence are of particular interest.[2] Excited molecules of this type can be deactivated by collisions with ground state triplet oxygen in a dynamic quenching process. The result is a reduction in luminescence intensity and lifetime dependent on the oxygen concentration according to the classic Stern-Volmer relationship, Equation 1, where "τ" is the lifetime, "I" is the emission intensity, k_q is the bimolecular quencher constant, and the 0 subscripts denote the value in the absence of oxygen. Luminescence quenching measurements are desirable because of their high sensitivity, high accuracy, and non-invasiveness. Further, they are highly compatible with

[*]corresponding author: fraser@virginia.edu.

imaging techniques enabling medical applications such as monitoring regenerating tissue, cancerous tumors, or chronic wounds.[3–7]

$$\frac{\tau_0}{\tau} = \frac{I_0}{I} = 1 + k_q \quad \tau_0\,[O_2] \qquad (1)$$

Sensors for luminescence quenching-based probes measure changes in either emission intensity or lifetime modes. While intensity sensing is generally simpler, it is dependent on measuring an unquenched reference signal. A reference is necessary because the intensity can be affected by external factors such as excitation noise, background fluorescence, probe concentration, scattering losses, and decomposition. The lifetime, however, is an intrinsic property of a molecule and thus remains unchanged by these factors. A great advantage of lifetime-based imaging is the independence of probe concentration, as this is problematic when probes accumulate in specific biological regions, such as tumors.[8] Thus, in the case of lifetime, a single oxygen calibration at a given temperature is necessary per probe, making it preferable for applications with dynamic environments.

Lifetime based oxygen imaging instruments are widespread due to the attractiveness of this parameter. Wang et al., for example, have created several systems capable of measuring spatially resolved lifetimes on the order of nanoseconds.[9–11] Decays on such a short time scale require sophisticated hardware resulting in increased complexity and immobility. Other simpler systems have been developed but are restricted to lifetimes on the microsecond scale and still require external gating control as well as image intensifiers, pulse generators, or cameras with ultra-fast shutters which can be costly.[12,13] For example, to monitor the phosphorescence lifetimes of ruthenium based dyes (1-5 μs) with complementary metal-oxide silicon camera (CMOS), both ultrafast shutters and image intensifiers are typically employed.[14,15] Indeed most lifetime imaging systems suffer from some combination of expense and complexity. Limitations become increasingly pronounced with faster lifetimes.

Technical demands, and thus cost, can be minimized by using long-lived probes. This approach is successful in phosphorescence lifetime imaging microscopy (PLIM) for background free imaging of cells and tissues.[16-18] These molecules eliminate the need for a fast excitation pulse and have the additional advantage of diminishing background interference from shorter-lived luminophores in the environment. However probes with lifetimes on the order of milliseconds or longer are few and far between. Certain trivalent europium and terbium complexes, as well as some metalloporphyrins, have lifetimes on this scale.[19,20] However, rare-earth and heavy metal activated phosphorescence materials can be costly and may lead to unintended cytotoxicity for the biological specimens.[21] In recent years, purely organic phosphors have been developed with exceptionally long lifetimes, but the phosphorescence is either oxygen insensitive due to material crystallinity[22–24] or dyes are embedded in biologically incompatible polymer matrices.[25,26] For biological sensing applications, dual emissive difluoroboron β-diketonate s conjugated to biodegradable polylactide (BF$_2$bdkPLA), have been developed.[27–29] Modifications to the dye scaffold, and polymer composition have enabled fabrication of oxygen sensitive films,[30] nanoparticles,[31]

and nanofibers.[32] These materials exhibit lifetimes up to hundreds of milliseconds making them uniquely compatible low cost imaging methods.

Many commercial oxygen sensing techniques based on luminescence already exist.[33] For example, ©Presens has developed a convenient hand-held system that utilizes the red/green/blue (RGB) channels of a camera to perform ratiometric imaging.[2] The hand-held camera, in combination "sensor foils" generates oxygen maps to gather spatial and temporal information. Commercial lifetime-based oxygen sensors are primarily fabricated as fiber optic lifetime decay O_2 sensors, such as the ©Piccolo$_2$ developed by ©PyroScience.[27] These provide highly reliable O_2 measurements, but only point measurements based on the location of the probe tip, and can be invasive in a biological context. Lifetime based measurements can be performed spatially with high-speed cameras, but dependent on the phosphors in use, costs and feasibility can differ greatly.

Recently, Meier et al. compared several camera-based imaging techniques. Of those reviewed, lifetime imaging was shown to be the most expensive ($15,000 - $60,000), the most complex, and the least portable.[34] We have substantially minimized these limitations with the system described below. Our setup costs less than $5000, easily fits into a backpack, and can operate on battery power alone. We report the development of a low-cost real-time oxygen imaging system that takes advantage of the long lifetimes of heavy-atom free BF_2bdkPLA materials. The lifetimes of four different boron polymer materials are measured and compared with those measured by a commercial phosphorimeter to determine accuracy and precision. Real-time imaging is also demonstrated. This study demonstrates great synergy between bright boron based probes with long phosphorescence lifetime and camera imaging techniques. It sets the stage for the future development of real time, combined lifetime and ratiometric imaging with more O_2 sensitive boron materials and their application in medicine.

Experimental Section

Method Concept

A digital camera is an ideal tool for two-dimensional analysis. At its core is an array of photosensors (pixels) that convert incident photons into a digital signal. Each pixel acts as its own sensing element providing spatial resolution, while a gated shutter provides temporal resolution. These processes are all performed on-board by the digital chip allowing for simple operation. Further, the commercialization of digital cameras has significantly reduced their price. The goal of this study is to utilize such a camera for quantitative lifetime imaging of oxygen levels.

Lifetimes are measured with our system by monitoring a luminescent probe with a camera. The sample is excited with pulsed UV light, and the subsequent decay is analyzed frame by frame via software. Because the gated shutter temporally resolves each frame, emission intensity may be determined as a function of time and fit to a decay function using nonlinear least squares (NLS), which yields the lifetime as a function of position. Filters, profile detection in software, and a comparatively fast pulse minimize contributions from the excitation pulse. Repeating this process pixel-wise may perform imaging. To achieve enough

data points for good NLS fits, the lifetime must be longer than the time between each frame. This prerequisite rules out most probes. However in the case of BF_2bdkPLA materials, even basic modern cameras have the necessary shutter speed.

If real-time imaging is desired, the rapid lifetime determination (RLD) method (see Figure S1), described by Ashworth et al., is employed in combination with our system instead of NLS.[35] This method requires that only two frames be captured. The lifetime is then calculated according to equation 2, where the integration times (t_1 and t_2) are given by the shutter speed and the integration values (A_1 and A_2) are calculated from pixel intensities within each frame. Unlike NLS, RLD has a closed form making it up to hundreds of times faster computationally. RLD can be performed pixel-wise in real-time where the imaging speed is limited only by the time between excitation pulses. Furthermore, because it requires fewer frames than does NLS, shorter lifetimes can be detected. RLD has been shown to demonstrate good accuracy and precision for single exponential decays even under low light conditions.[36] However in the multiexponential case, it should be noted that the accuracy of the calculations can change depending on how the integration intervals (t_1 and t_2) are selected.

$$\tau = \frac{t_2 - t_1}{ln\left(\frac{A_1}{A_2}\right)}$$

(2)

System Setup and Components

A schematic of the system setup is shown in Figure 1. Samples are placed approximately 0.5 m below the camera and are excited by a manually triggered Yongnou 560-II flash unit masked by an Esco Optics 425 nm bandpass filter (40 nm bandwidth). Pulses with reproducible profiles and durations as short as 50 μs can be generated at regular intervals for imaging. Images are captured with a PGR GS3-U3-41C6C-C video camera (http://www.ptgrey.com/) equipped with a Spacecom f/0.95 50 mm lens and an Edmund Optics 425 nm long pass filter to minimize excitation background. Emission profiles of filters used are shown in Figure S2. The camera has a color CMOS chip capable of 90 frames per second (FPS) at a maximum resolution of 2048×2048 pixels. Framerates up to 2000 FPS can be achieved at reduced resolutions. A color camera was chosen to increase versatility for other luminescence-based applications. The quantum efficiencies of the color channels are shown in Figure S3. Camera data and power are provided through a USB 3.0 cable connected to a Lenovo w530 laptop, which is responsible for camera control, data acquisition, processing, and display. Further details about component selection and cost are provided in Table S1. All components can easily fit in a backpack for portability and can operate on battery power for field applications.

Software Design

The camera records 8-bit Bayer data and performs a nearest-neighbor demosaicing algorithm on-board unless otherwise specified. Camera control, data acquisition, processing, and display are all performed in custom MATLAB 2014b programs. The Image Acquisition and Curve Fitting toolboxes are necessary add-ons for these programs. The apparent light

intensity is controlled primarily through the shutter speed. Gain may be increased if the image is underexposed. Otherwise it is turned off. Gamma correction is always set to a value of 1 (meaning no additional amplification or distortion of the sensor output is applied). The white balancing feature is also turned off. The region of interest (ROI) may be specified to reduce data output or increase framerate. The FPS is set based on the calculation method (NLS vs RLD) as well as the range of expected lifetimes. Total intensity at a single pixel is determined by summing the 8-bit values from red, green, and blue channels.

If single, absolute lifetime measurements are desired, the NLS method is used and the FPS is set such that at least ten frames will be acquired during the decay. The beginning of the decay is detected in software by the appearance of the excitation peak. After monitoring the decay, all pixel intensities in the ROI are averaged frame-by-frame and fit as a function of time (determined by the FPS) to a single or multiexponential decay function with an offset. In the case of a single exponential decay, the lifetime may be extracted directly from the fit parameters. For a multiexponential decay, a weighted lifetime is calculated using pre-exponential weighting.[37] Oxygen imaging may be performed by computing the lifetime at each pixel, applying a predetermined oxygen calibration, and displaying the resultant distribution as a scaled colormap. This process is computationally intensive and cannot be done in real time. It should also be noted that precision in general decreases as fewer pixels are averaged.

For high speed imaging applications, the RLD method is used. A simplified flow chart of the processing is shown in the right hand side of Figure 1. The FPS is set such that at least two frames will be acquired during the decay. Because an offset can significantly affect the ratio of the denominator of the RLD equation, a background image is captured before imaging begins. The excitation pulse is detected in software and at least two consecutive frames are subsequently captured. The background image is subtracted pixel-wise from each frame. The lifetime at each pixel is then determined by Equation 2 where the numerator is the inverse framerate and the denominator is given by the natural logarithm of the ratio of intensities. A predetermined oxygen calibration is then applied to each pixel to determine the concentration. The oxygen distribution is displayed as a scaled colormap. The program then awaits the next excitation pulse. The program used for RLD imaging is available in Figure S4. Because the decay times are substantially longer than the RLD processing time, real time processing may be performed at full resolution at 2 FPS. If lifetimes are long enough to capture more than two frames, the width and timing of the integration intervals may be changed in software for optimal performance.

Materials

Boron dyes were prepared as previously described.[27,28,38] Steady-state fluorescence emission spectra were recorded on a Horiba Fluorolog-3 Model FL3-22 spectrofluorometer (double-grating excitation and double-grating emission monochromator). A 2 ms delay was used when recording the long-lived emission spectra. Phosphorescence lifetimes were measured with a 1 ms multichannel scalar (MCS) excited with a flash xenon lamp (λex = 369 nm; bandwidth = 5 nm; duration <1 ms). Lifetime data were analyzed with DataStation v2.4 software from Horiba Jobin Yvon. Oxygen sensitivity calibrations were performed as

previously described.[28] Thin films were prepared on the inner wall of vials by dissolving polymers in CH_2Cl_2 (5 mg/mL) and then evaporating the solvent by slowly rotating the vial under a slow stream of nitrogen. The films were then dried in vacuo for at least ~15 min before measurements were taken.

Results and Discussion

Photophysical Properties

Non-heavy atom substituted BF_2bdkPLA materials were chosen to demonstrate imaging system capability because of their long phosphorescence lifetimes at room temperature, shown in Figure 2. Specifically, polymers with molecular weights (MWs) of 15 kDa or higher were selected because of their long phosphorescence lifetimes (117-265 ms). The delayed emission of BF_2bdkPLA polymers is comprised of room temperature phosphorescence (RTP) and thermally activated delayed emission (TADF) at room and body temperatures.[31] Samples **1** (BF_2dbmPLA, 20 kDa) and **2** (BF_2nbmPLA, 19 kDa) show predominantly RTP, while BF_2dnmPLA polymers (sample **3**, 30 kDa and sample **4**, 16 kDa) show more significant TADF.[27] Because TADF is a thermal process, the delayed emission color, lifetime, and oxygen sensitivity[39] change dramatically with variations in temperature.[38] BF_2nbmPLA (**2**) polymers have the largest singlet-triplet gaps (465-545 nm), and long unquenched phosphorescence lifetimes (222 ms), making this dye scaffold optimal for long-lived phosphorescence applications.[26,39,40] All polymers **1-4** have long-lived triplet emissions, resulting in hypersensitivity to oxygen quenching. Because these dyes are covalently linked to the polymer matrix, fabrication into nanoprobes is easily achieved for biomedical application to acquire spatial information.[31,41]

System Performance

A linear output is essential to obtaining quantitative data from digital cameras. Nonlinearity is common in lower cost cameras and may arise during multiple stages between when photons strike the sensor and when the image is displayed. While the sensor itself can be nonlinear and heterogeneous, the raw signal is usually distorted most by software. Some sources of nonlinearity include gamma, white balance, brightness, and compression. The issue is further complicated in the case of color cameras which have different filters covering every pixel and require an additional processing step (demosaicing) to extract color images. To ensure that the response of our system was reliable, a linearity calibration using neutral density filters was performed. The results (see Figure S5) show that all three color channels, as well as "total emission" determined by summing all three, show excellent linearity.

Once linearity was confirmed, we tested the performance of our system with BF_2bdkPLA materials. The lifetimes of four derivatives including BF_2dbmPLA (**1**), BF_2nbmPLA (**2**) and BF_2-dnmPLA (**3**, 16 kDa and **4**, 30 kDa) were measured under nitrogen using NLS and RLD. These unquenched lifetimes were compared with those measured by a commercial phosphorimeter used as the standard. The results are shown in Table 1. Lifetimes determined by NLS at a framerate of 90 FPS demonstrated high accuracy and precision, obviating the need for additional oxygen calibrations specific to our system. RLD performed similarly, however because the lifetimes of the materials used in this study are multiexponential, it was

necessary to choose optimum integration parameters for each dye. Details of these parameters are given in Table S2. Due to the limited frame rate of our system, a rapid decrease in accuracy and precision was observed for lifetimes shorter than 1 ms using NLS or 200 μs using RLD.

Dynamic Imaging Application

The real-time oxygen imaging capability of the system when applied to BF_2bdk materials was demonstrated. The oxygen sensitivity of **2** was calibrated using a spectrofluorimeter (Figure 3). Polymer $BF_2nbmPLA$ (**2**) (~5 mg dissolved in CH_2Cl_2) was drop-cast onto a glass surface to create a film of variable thickness. A stream of nitrogen gas was then blown onto the surface as continuous RLD imaging was performed using 55 ms integration intervals and a two second delay between excitation pulses. The raw intensity profile of an ROI and the associated spatially resolved frames are shown in Figure 3. Images from a higher time resolution repeated trial of this experiment with a shorter delay between pulses are shown in Figure S6.

Conclusions

An economical spatiotemporally resolved oxygen-imaging system was presented. It utilizes especially long lived oxygen sensitive probes, significantly reducing the technical demands of instrumentation. Our system improves upon three major limitations to typical lifetime based oxygen sensing (complexity, portability, and cost) and is also capable of imaging in real time. Both NLS and RLD lifetime calculation methods may be employed and each are suited to different scenarios. The camera can detect lifetimes as short as 200 μs. We tested the performance of the camera imaging system with four BF_2bdk samples. The lifetimes of these probes were measured and shown to be accurate and precise. Then, real-time oxygen imaging was demonstrated using a heterogeneous film of sample **2**. The versatility of the imaging system combined with the biocompatibility of BF_2bdk materials provides a cost effective alternative for oxygen visualization in biological systems. Imaging systems can also be expanded to even simpler capturing devices, such as handheld camera phones.[42] Further system optimization, development of simultaneous lifetime and ratiometric imaging, and biomedical applications testing with BF_2bdk probes are underway and will serve as the subjects of future reports.

Supplementary Material

Refer to Web version on PubMed Central for supplementary material.

Acknowledgements

Notes and references

1. Giaccia AJ, Simon MC, Johnson R. Genes Dev. 2004; 18:2183–94. [PubMed: 15371333]
2. Wang X, Wolfbeis OS. Chem. Soc. Rev. 2014; 43:3666–761. [PubMed: 24638858]

3. Kannan RY, Salacinski HJ, Sales K, Butler P, Seifalian AM. Biomaterials. 2005; 26:1857–1875. [PubMed: 15576160]

4. Phelps EA, García AJ. Curr. Opin. Biotechnol. 2010; 21:704–9. [PubMed: 20638268]

5. Hockel M, Vaupel P. JNCI J. Natl. Cancer Inst. 2001; 93:266–276. [PubMed: 11181773]

6. Harris AL. Nat. Rev. Cancer. 2002; 2:38–47. [PubMed: 11902584]

7. Bishop A. J. Wound Care. 2008; 17:399–402. [PubMed: 18833899]

8. Zheng X, Wang X, Mao H, Wu W, Liu B, Jiang X. Nat. Commun. 2015; 6:5834. [PubMed: 25556360]

9. Wang XF, Kitajima S, Uchida T, Coleman DM, Minami S. Appl. Spectrosc. 1990; 44:25–30.

10. Wang XF, Uchida T, Coleman DM, Minami S. Appl. Spectrosc. 1991; 45:360–366.

11. Wang XF, Uchida T, Minami S. Appl. Spectrosc. 1989; 43:840–845.

12. Shonat RD, Wilson DF, Riva CE, Pawlowski M. Appl. Opt. 1992; 31:3711–8. [PubMed: 20725344]

13. Liebsch G, Klimant I, Frank B, Holst G, Wolfbeis OS. Appl. Spectrosc. 2000; 54:548–559.

14. Hirvonen LM, Festy F, Suhling K. Opt. Lett. 2014; 39:5602–5605. [PubMed: 25360938]

15. Hirvonen LM, Petrášek Z, Beeby A, Suhling K. New J. Phys. 2015; 17:023032.

16. Baggaley E, Botchway SW, Haycock JW, Morris H, Sazanovich IV, Williams JAG, Weinstein JA. Chem. Sci. 2014; 5:879–886.

17. Jenkins J, Dmitriev RI, Papkovsky DB, Becker W. Advanced Time-Correlated Single Photon Counting Applications, Springer Series in Chemical Physics. Imaging Cell and Tissue O$_2$ by TCSPC-PLIM. 2015; 111

18. Becker, W.; Su, B.; Bergmann, A.; Weisshart, K.; Holub, O. Proc. SPIE 7903, Multiphoton Microscopy in the Biomedical Sciences XI. Periasamy, Ammasi; König, Karsten; Peter, TC., editors. San Francisco, California, USA: 2011. p. 790320790320

19. Li Z, Roussakis E, Koolen PGL, Ibrahim AMS, Kim K, Rose LF, Wu J, Nichols AJ, Baek Y, Birngruber R, Apiou-Sbirlea G, Matyal R, Huang T, Chan R, Lin SJ, Evans CL. Biomed. Opt. Express. 2014; 5:3748–64. [PubMed: 25426308]

20. Hanaoka K, Kikuchi K, Kobayashi S, Nagano T. J. Am. Chem. Soc. 2007; 129:13502–9. [PubMed: 17927176]

21. Zhao Q, Huang C, Li F. Chem. Soc. Rev. 2011; 40:2508–24. [PubMed: 21253643]

22. Gong Y, Zhao L, Peng Q, Fan D, Yuan WZ, Zhang Y, Tang BZ. Chem. Sci. 2015; 6:4438–4444.

23. An Z, Zheng C, Tao Y, Chen R, Shi H, Chen T, Wang Z, Li H, Deng R, Liu X, Huang W. Nat. Mater. 2015; 14:685–90. [PubMed: 25849370]

24. Bolton O, Lee K, Kim H-J, Lin KY, Kim J. Nat. Chem. 2011; 3:205–10. [PubMed: 21336325]

25. Lehner P, Staudinger C, Borisov SM, Regensburger J, Klimant I. Chem. Euro. J. 2015; 21:3978–86.

26. Lehner P, Staudinger C, Borisov SM, Klimant I. Nat. Commun. 2014; 5:4460. [PubMed: 25042041]

27. DeRosa CA, Samonina-Kosicka J, Fan Z, Hendargo HC, Weitzel DH, Palmer GM, Fraser CL. Macromolecules. 2015; 48:2967–2977. [PubMed: 26056421]

28. DeRosa CA, Kerr C, Fan Z, Kolpaczynska M, Mathew AS, Evans RE, Zhang G, Fraser CL. ACS Appl. Mater. Interfaces. 2015; 7:23633–43. [PubMed: 26480236]

29. Zhang G, Palmer GM, Dewhirst MW, Fraser CL. Nat. Mater. 2009; 8:747–751. [PubMed: 19668206]

30. Zhang G, Chen J, Payne SJ, Kooi SE, Demas JN, Fraser CL. J. Am. Chem. Soc. 2007; 129:8942–8943. [PubMed: 17608480]

31. Pfister A, Zhang G, Zareno J, Horwitz AF, Fraser CL. ACS Nano. 2008; 2:1252–1258. [PubMed: 19081748]

32. Bowers DT, Tanes ML, Das A, Lin Y, Keane NA, Neal RA, Ogle ME, Brayman KL, Fraser CL, Botchwey EA. ACS Nano. 2014; 8:12080–91. [PubMed: 25426706]

33. Wolfbeis OS. BioEssays. 2015; 37:921–928. [PubMed: 26113255]

Author Manuscript

Author Manuscript

Author Manuscript

Author Manuscript

34. Meier RJ, Fischer LH, Wolfbeis OS, Schäferling M. Sensors Actuators B Chem. 2013; 177:500–506.

35. Ashworth A, Woods RJ, Scypinski S, Love LJC. Anal. Chem. 1984; 56:1395–1400. [PubMed: 6465515]

36. Ballew RM, Demas JN. Anal. Chem. 1989; 61:30–33.

37. Carraway ER, Demas JN, DeGraff BA. Anal. Chem. 1991; 63:332–336.

38. Payne SJ, Zhang G, Demas JN, Fraser CL, Degraff BA. Appl. Spectrosc. 2011; 65:1321–1324. [PubMed: 22054093]

39. Kochmann S, Baleizão C, Berberan-Santos MN, Wolfbeis OS. Anal. Chem. 2013; 85:1300–1304. [PubMed: 23320578]

40. Palmeira T, Fedorov A, Berberan-Santos MN. Methods Appl. Fluoresc. 2014; 2:035002.

41. Kerr CA, de la Rica R. Anal. Methods. 2015; 7:7067–7075.

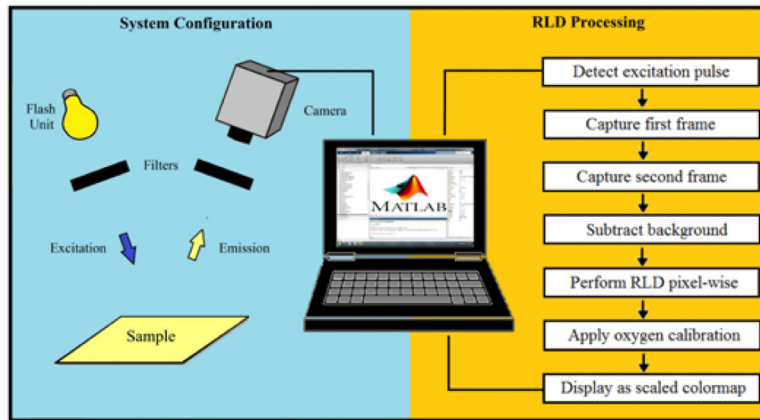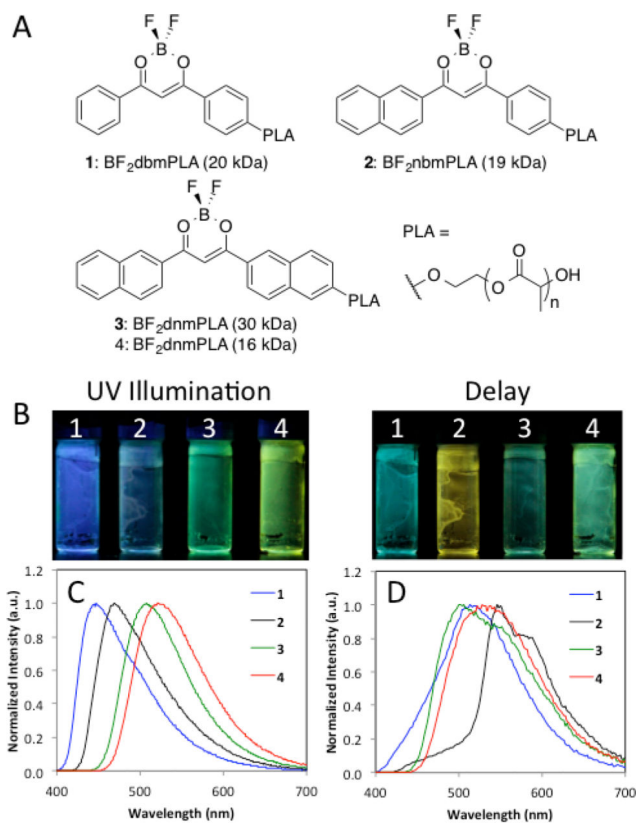42. O'Driscoll S, MacCraith BD, Burke CS. Anal. Methods. 2013; 5:1904.

Figure 1.
Schematic of the system setup (left) and data processing for real time RLD imaging (right)

Figure 2.
Optical properties of BF$_2$bdkPLA materials. a) Structures and nomenclature of boron dye PLA materials. b) Image of dye-PLA polymers under nitrogen with continuous UV illumination (λ_{ex} = 365 nm) showing fluorescence plus phosphorescence and delayed image; λ_{ex} = camera flash with blue filter (i.e. phosphorescence plus thermally activated delayed fluorescence) c) Total emission spectra in air (λ_{ex} = 369 nm). d) Delayed emission spectra under nitrogen (λ_{ex} = 369 nm)
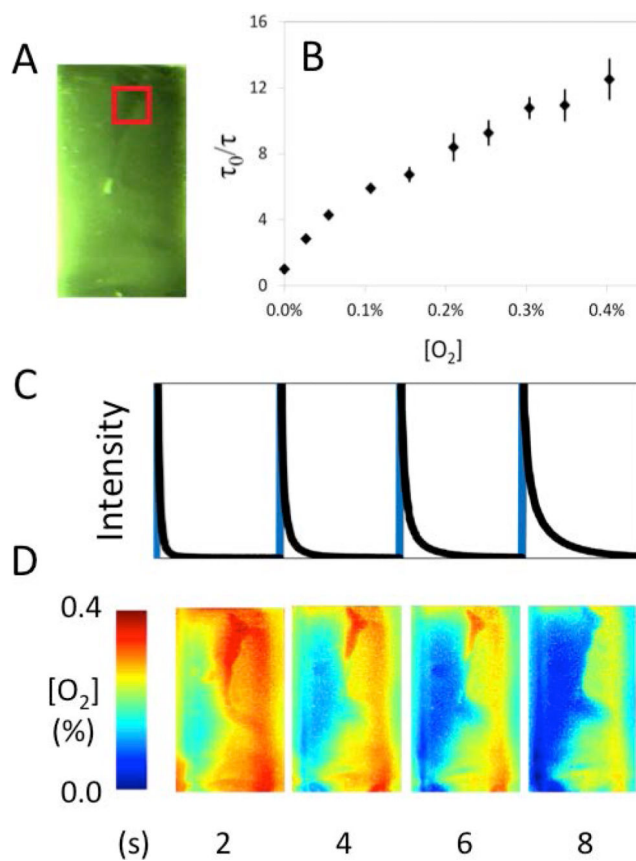
Figure 3.
Imaging demonstration of a vial containing a film of **2** being purged with a stream of nitrogen showing a) Image of phosphorescence with the region of interest (ROI) highlighted in a red box, b) Stern-Volmer calibration plot and c) raw camera intensity plot of an ROI during imaging (detected excitation in blue, sample decay in black) aligned with d) the fully processed oxygen color maps.

Table 1

Phosphorescence Lifetime (τ_P) Comparison

Sample	MSPC[a] (ms)	NLS[b] (ms)	RLD[c] (ms)
1	265 ± 2	253 ± 21	256 ± 23
2	222 ± 7	216 ± 19	228 ± 8
3	203 ± 1	209 ± 7	193 ± 8
4	117 ± 1	119 ± 4	114 ± 1

[a] Multi-scalar photon counting (Horiba fluorimeter)

[b] Non-linear least squares (NLS)

[c] Rapid lifetime determination (RLD). Uncertainties are the standard deviation for three independent measurements